Free-Radical Polymerization Kinetics of 2-Acrylamido-2-methylpropanesulfonic Acid in Aqueous Solution

Sabine Beuermann,*,† Michael Buback,† Pascal Hesse,† Thomas Junkers,† and Igor Lacík‡

Institute of Physical Chemistry, Georg-August-University, Tammannstrasse 6, D-37077, Göttingen, Germany, and Polymer Institute of the Slovak Academy of Sciences, Dúbravská cesta 9, 842 36 Bratislava, Slovak Republic

Received June 7, 2005; Revised Manuscript Received November 7, 2005

ABSTRACT: The SP−PLP−NIR technique, which combines pulsed laser polymerization (PLP) initiated by a single pulse (SP) with time-resolved monitoring of the resulting monomer conversion via near-infrared (NIR) spectroscopy, was used to investigate the kinetics in aqueous solution of 2-acrylamido-2-methylpropanesulfonic acid (AMPS). For initial AMPS concentrations of 2.79 mol·L^{-1} (50 wt % AMPS) and 1.04 mol·L^{-1} (20 wt % AMPS), the ratio of (chain length averaged) termination and propagation rate coefficients, $\langle k_t \rangle / k_p$, was measured up to almost complete monomer conversion at temperatures between 10 and 40 °C and ambient pressure. Up to 80% monomer conversion, $\langle k_t \rangle / k_p$ is only slightly lowered, whereas there is a clear decrease upon further increasing conversion. Variation of temperature and of pH does not significantly affect $\langle k_t \rangle / k_p$. For estimating individual rate coefficients, $\langle k_t \rangle$ and k_p, in addition chemically initiated polymerizations have been carried out, in which AMPS conversion was monitored via in-line FT-NIR spectroscopy. The resulting $\langle k_t \rangle$ and k_p values, for 40 °C and an initial AMPS concentration of 2.79 mol·L^{-1}, are 2×10^7 L·mol^{-1}·s^{-1} and 1×10^5 L·mol^{-1}·s^{-1}, respectively. Both rate coefficients are significantly higher at the lower AMPS content of 1.04 mol·L^{-1}. $\langle k_t \rangle$ at this lower AMPS content may be understood in terms of termination occurring under reaction diffusion control. The lowering in rate coefficients measured at the higher AMPS content is indicative of a reduced poly(AMPS) chain mobility.

Introduction

During recent years, the understanding of radical polymerization kinetics and mechanism has largely improved on the basis of accurate rate coefficients deduced via pulsed laser polymerization (PLP) experiments.[1] Detailed information on termination rate coefficients, k_t, may be obtained by the SP−PLP−NIR technique, in which polymerization induced by a single pulse (SP) is monitored via near-infrared (NIR) spectroscopy with microsecond to millisecond time resolution.[2] The technique was first applied to ethene high-pressure polymerization[2] and was then extensively used for studies into homo- and copolymerization kinetics of (meth)acrylate monomers[3,4] including investigations into the chain-length dependence of k_t.[5] The method was mostly applied to bulk polymerizations, but also to measure k_t in mixtures with supercritical carbon dioxide.[6] Actually, the SP−PLP−NIR trace, which represents the time evolution of conversion after applying a laser pulse at $t = 0$, yields the ratio of termination to propagation rate coefficients, k_t/k_p. As radical chain length increases with time t, this notation refers to the idealized situation of both k_t and k_p being independent of chain length. Whereas k_p depends on chain length only at small radical sizes,[7] k_t may significantly vary with chain length over a wide range of free-radical size. Depending on the kinetic model underlying the analysis of the SP−PLP−NIR trace, the termination rate coefficient is deduced either as a mean value, $\langle k_t \rangle$, over time and free-radical chain length or as chain-length dependent k_t. If k_p is known from the so-called PLP−SEC technique,[8] which combines PLP and subsequent analysis of the polymer molecular weight distribution by size-exclusion chromatography (SEC), termination rate coefficients are deduced from the coupled parameters, $\langle k_t \rangle / k_p$ or k_t/k_p, obtained via SP−PLP−NIR.

Most of the PLP−SEC work carried out so far has addressed oil-soluble monomers,[1] in particular those that yield polymeric material that may be dissolved in the standard SEC eluent THF. Water-soluble monomers have been less frequently studied by PLP−SEC despite the numerous applications of the associated polymers, e.g., in the preparation and modification of hydrogels, membranes, biomedical devices, flocculants, and stabilizers of nanoparticles. Only recently, reliable k_p data from PLP−SEC were reported for aqueous-phase polymerizations of *N*-isopropylacrylamide,[9] acrylamide,[10] methacrylic acid,[11] and acrylic acid.[12−14] SP−PLP−NIR studies into the termination behavior of water-soluble monomers have not been carried out so far, with the exception of acrylic acid, which is currently under investigation in our group.

The present paper focuses on measuring rate coefficients of 2-acrylamido-2-methylpropanesulfonic acid (AMPS) polymerization in aqueous solution. AMPS belongs to a group of monomers that are highly acidic. Though the associated polymer is of technical relevance, e.g., as a hydrogel material,[15] kinetic data derived from PLP experiments are not yet available. First attempts to obtain k_p via the PLP−SEC method were not successful.[16] We thus replaced the combination of PLP−SEC and SP−PLP−NIR experiments, which has mostly been used for deducing individual termination rate coefficients, by SP−PLP−NIR measurements carried out in conjunction with chemically initiated polymerizations, which latter experiments yield $k_p/\langle k_t \rangle^{0.5}$. The termination rate coefficients reported in what follows are time-averaged and chain-length-averaged quantities.[17] Kinetic measurements were performed at moderate temperature variation, between 10 and 40 °C, and upon changing pH, by adding NaOH, such that AMPS and the associated sodium salt are polymerized.

* Corresponding author. E-mail: sbeuerm@gwdg.de.
† Georg-August-University.
‡ Slovak Academy of Science.

10.1021/ma051187n CCC: $33.50
Published on Web 12/21/2005

Scheme 1. 2-Acrylamido-2-methylpropanesulfonic Acid (AMPS)

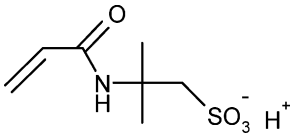

Experimental Section

Chemicals. The monomer 2-acrylamido-2-methylpropanesulfonic acid (AMPS; Fluka, ≥97%), depicted in Scheme 1, was recrystallized from methanol to remove impurities. The photoinitiator 2-hydroxy-2,2-dimethyl acetophenone (Darocur 1173, Merck), the thermally decomposing initiator sodium peroxodisulfate (Fluka, ≥99%), deuterium oxide (D_2O; Deutero GmbH, 99.9%), methanol (Merck, >99.8), and NaOH (Scharlau, > 99%) were used as received. Demineralized water was used to prepare the aqueous monomer solutions and the NaOH solutions.

Preparation of the Solutions for Polymerization. AMPS, Darocur 1173, and water were mixed in a 5 mL flask. Typical initial concentrations of Darocur 1173 and AMPS were $c_{\text{Darocur}} = 5 \times 10^{-3}$ mol·L^{-1} and $c_{\text{AMPS}} = 2.79$ mol·L^{-1} (50 wt %), respectively. To remove oxygen, the monomer mixture was purged with nitrogen for 5 min. The solution was then filled into the polymerization cell consisting of a Teflon tube closed by a cylindrical quartz window on each side. This internal cell was fitted into a stainless steel cell of transmission type equipped with two sapphire windows. Details of the experimental setup including heating and temperature control are given elsewhere.[18] To promote heat transfer to the internal cell, the stainless steel cell was filled with *n*-heptane.

Aqueous NaAMPS solutions were prepared by neutralization of solid AMPS with 6 M aqueous NaOH. The monomer was weighed into a volumetric flask. The aqueous NaOH stock solution was added under ice cooling. The pH was measured using a Metrohm 602 pH meter after the addition of the NaOH solution. Details about the preparation of initial mixtures for free-radical polymerization in aqueous phase are given elsewhere.[13]

SP−PLP−NIR Experiments. The change in AMPS concentration due to laser-induced polymerization was measured with time resolution in the microsecond range. The SP−PLP−NIR setup consisted of an excimer laser (Lextra 50, Lambda Physik) with a pulse width of 20 ns operated on the XeF line at 351 nm, a 75 W tungsten halogen lamp (General Electric) powered by two batteries (12 V, 180 A h), a BM 50 monochromator (B&M Spectronic), and a detector unit equipped with a fast InAs detector (EG & G, Judson) of 2 μs time resolution. The PC for data acquisition was equipped with a transient recorder card (16 bit TR 1621-4, Fast ComTec). The stainless steel cell was positioned between the tungsten lamp and the InAs detector.[2] The aqueous monomer−photoinitiator solution was irradiated with excimer laser light of 1 mJ energy per pulse. The pulse-induced variation in monomer concentration was associated with a change in transmitted light intensity at the monomer peak position around 6173 cm^{-1}.

In between each single-pulse experiment, the stainless steel cell was inserted into the sample compartment of an FT-IR/NIR spectrometer (IFS 88, Bruker) to measure the entire NIR spectrum. Via the NIR spectra taken before applying the laser pulse and after pulse-induced polymerization has ceased, the light intensities at the monomer peak position, which actually are voltage signals recorded with high time resolution, were calibrated and converted into monomer concentration vs time *t* traces. The FT-NIR spectrometer is equipped with a silicon-coated CaF_2 beamsplitter, a halogen lamp, and an InSb detector. The sequence of time-resolved (SP−PLP−NIR) measurement at a fixed wavenumber and of FT-NIR detection of AMPS concentration via the entire NIR spectrum was repeated until almost complete monomer conversion was reached. Up to around 90% monomer conversion, data analysis was performed for true single pulse traces. At even higher conversions, up to four measured single pulse traces were co-added to improve signal-to-noise quality (see below).

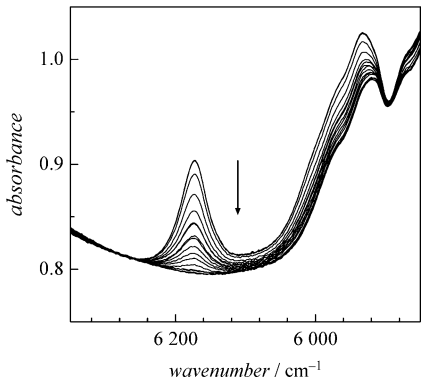

Figure 1. FT-NIR spectra series recorded during 2-acrylamido-2-methylpropanesulfonic acid (AMPS) polymerization in H_2O at 40 °C, ambient pressure, and initial AMPS concentration of 2.79 mol·L^{-1}. The arrow indicates the direction of absorbance change during polymerization.

Size-Exclusion Chromatography. The aqueous-phase SEC setup consisted of a Waters in-line degasser, a Waters pump 515 equipped with a plunger washing kit, a Rheodyne 7725i injector, a guard, and three Suprema columns (Polymer Standards Service) of particle size 10 μm and pore sizes of 100, 1000, and 3000 Å (positioned in a Waters column heater module). The analyses was performed at 60 °C using demineralized water as the eluent, which contained 0.1 mol·L^{-1} Na_2HPO_4, to provide a pH value of 9.0, and 200 ppm NaN_3. The eluent was permanently stirred to avoid concentration changes as a consequence of salt sedimentation. Ethylene glycol was used as the flow marker to adjust eluent flow to a rate of 1 mL·min^{-1}. To obtain absolute molecular weights, the SEC setup was equipped with a differential refractometer (Waters M2410) and a MALLS detector (Polymer Standards Service PSS SLD7000), with d*n*/d*c* of 0.137 mL·g^{-1} determined at 633 nm using a Brice-Phoenix 2000-V differential refractometer. The poly(AMPS) samples were dissolved in the eluent at a concentration of 2 mg·mL^{-1} and filtered through a 0.45 μm filter. The injected volume was 200 μL. Data acquisition and analysis were performed via the WinGPC7.2 software (Polymer Standards Service).

Chemically Initiated Polymerizations. Monomer, sodium peroxodisulfate, and water were mixed in a 5 mL flask and purged with nitrogen under ice cooling for 3 min. The mixture was filled into the internal Teflon−quartz cell, which was fitted into the stainless steel cell that was already heated to polymerization temperature. The stainless steel cell was inserted into the sample compartment of the FT-IR/NIR spectrometer, and a series of NIR spectra was taken at preselected times until complete monomer conversion was reached. The determination of AMPS concentration from the FT-NIR spectra is described below. As an example, AMPS polymerizations in water with initial monomer and sodium peroxodisulfate concentrations of 2.79 and 0.02 mol·L^{-1}, respectively, were carried out at 40 °C and ambient pressure. NIR spectra were recorded every 30 s. After 22 min a monomer conversion of 90% was achieved. The polymer obtained has a weight-average molecular weight of 2.3×10^6 g·mol^{-1}.

Results and Discussion

In-Line FT-NIR Spectroscopy. In-line monitoring of chemical reactions via FT-NIR spectroscopy is well established in our group[19] and has been extensively used for quantitative analysis in nonaqueous systems.[19,20] Figure 1 shows a series of NIR spectra recorded during an AMPS polymerization in aqueous solution at 40 °C, ambient pressure, and an initial AMPS concentration of 2.79 mol·L^{-1}, corresponding to 50 wt % AMPS. The peak around 6173 cm^{-1} is assigned to the first overtone of the C−H stretching vibration at the C═C double bond of AMPS. The arrow indicates the direction of absorbance change during polymerization. The final spectrum was taken at

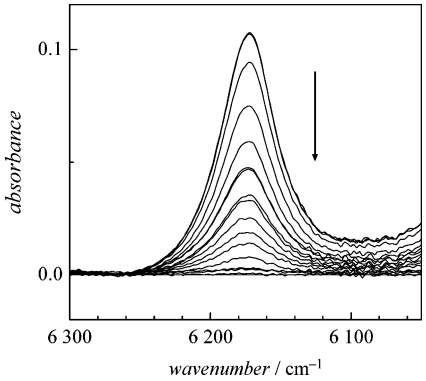

Figure 2. FT-NIR spectra deduced from the spectral series shown in Figure 1 by subtraction of the spectrum for complete 2-acrylamido-2-methylpropanesulfonic acid conversion from each of the individual absorbance spectra. The arrow indicates the direction of absorbance change during polymerization.

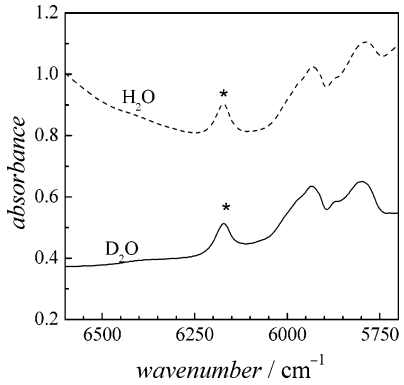

Figure 3. NIR spectra of 2.79 mol·L^{-1} 2-acrylamido-2-methylpropanesulfonic acid (AMPS) in solutions of D_2O (solid line) and H_2O (dashed line) at 40 °C and ambient pressure. The asterisks indicate AMPS peak positions.

almost complete monomer conversion. The background absorbance is due to H_2O combination bands. To estimate AMPS concentrations from the NIR spectra, the background absorbance was eliminated by subtraction of the spectrum for complete AMPS conversion from each spectrum taken during the course of the polymerization reaction (Figure 1). The resulting spectral series is shown in Figure 2. Monomer concentration was estimated via the high-wavenumber half-band that is obtained by integration from the peak position around 6173−6265 cm^{-1} against a horizontal baseline through the absorbance point at 6265 cm^{-1}.

The intense H_2O background absorbance poses problems toward quantitative NIR-spectroscopic AMPS analysis at lower monomer concentrations because of an unfavorable signal-to-noise ratio. Using D_2O instead of H_2O as the solvent should shift H_2O stretching modes to lower wavenumbers and thus may reduce background absorbance. Shown in Figure 3 are NIR spectra for AMPS in solution of D_2O (solid line) and H_2O (dashed line) under otherwise identical conditions of 40 °C, ambient pressure, and an AMPS concentration of 2.79 mol·L^{-1}. The asterisks indicate the peak position of the first C−H stretching overtone of AMPS. The strong water absorbance above 6300 cm^{-1} is not observed in D_2O solution. The background absorption in the case of D_2O has significantly dropped, from 0.8 to about 0.4 absorbance unit. The AMPS peak around 6173 cm^{-1} has not been affected upon replacing H_2O by D_2O. Using D_2O as the solvent, instead of H_2O, is thus advantageous, because the ratio of AMPS to water absorbance is enhanced and the signal-to-noise quality of the SP−PLP−NIR experiment is improved. Replacing H_2O by D_2O is particularly recommendable for experiments at low AMPS contents.

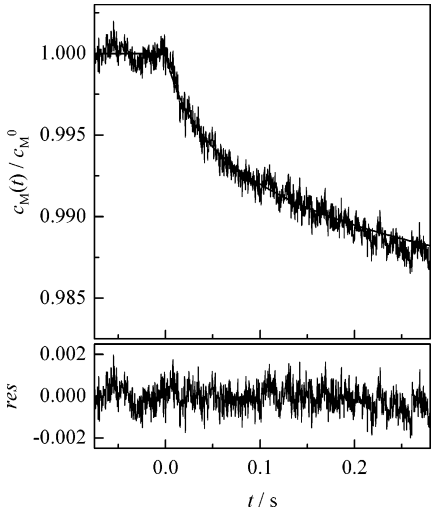

Figure 4. Change in relative monomer concentration, c_M/c_M^0, after applying an excimer laser pulse, at $t = 0$, during 2-acrylamido-2-methylpropanesulfonic acid (AMPS) polymerization in aqueous phase at 40 °C. This particular SP−PLP−NIR experiment has been carried out during AMPS polymerization with initial monomer concentration of 2.79 mol·L^{-1}. Monomer conversion at $t = 0$, due to the action of preceding laser pulses, is 43% (see text). The difference between measured and fitted (to eq 1) data is illustrated by plotting the residuals (res) in the lower part of the figure.

It is not to be expected that D_2O affects free-radical polymerization of AMPS in a way different from that of H_2O. This assumption has been tested by carrying out SP−PLP−NIR experiments on AMPS dissolved in H_2O and in D_2O under otherwise identical polymerization conditions.

Determination of $\langle k_t \rangle / k_p$ from SP−PLP−NIR Experiments. Shown in the upper part of Figure 4 is the monomer concentration vs time trace obtained during an SP−PLP−NIR experiment at 40 °C. The initial AMPS concentration was 2.79 mol·L^{-1}. The monomer conversion from the preceding PLP is 43%. The particular SP−PLP−NIR experiment illustrated in Figure 4 thus is carried out on a system that contains 57% of the initial monomer, which corresponds to an AMPS concentration of $c_M^0 = 1.6$ mol·L^{-1} at time $t = 0$ when the excimer laser pulse hits the sample. The horizontal pre-trigger region indicates that changes in monomer concentration due to the action of the preceding laser pulse have ceased. About 0.15 s after firing the laser pulse, relative AMPS concentration has decreased by about 1%, to $c_M/c_M^0 = 0.99$, as a consequence of PLP.

The experimental trace in Figure 4 is fitted to eq 1, which refers to idealized single pulse kinetics[1] on the basis of the termination rate law: $r_t = -2k_t c_R^2$. Termination occurs between two radicals of almost identical size *i*, with *i* increasing linearly with time *t* after applying the laser pulse at $t = 0$. To indicate that termination kinetics is chain length dependent, k_t in eq 1 has been replaced by $\langle k_t \rangle$. The expression for the change of relative monomer concentration with time *t* reads:

$$\frac{c_M(t)}{c_M^0} = (2\langle k_t \rangle c_R^0 t + 1)^{-k_p/2\langle k_t \rangle} \qquad (1)$$

in which c_R^0 is the radical concentration generated by instantaneous photoinitiator decomposition due to the action of the excimer laser pulse; c_M^0 is the monomer concentration prior

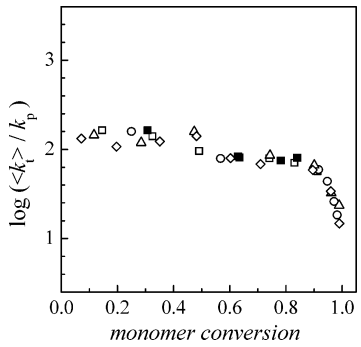

Figure 5. Dependence of $\langle k_t \rangle / k_p$ on monomer conversion deduced from SP−PLP−NIR experiments on 2-acrylamido-2-methylpropanesulfonic acid (AMPS) in aqueous solution of initial monomer concentration of 2.79 mol·L^{-1} and initiator concentration of $c_{\text{Darocur}} = 5 \times 10^{-3}$ mol·L^{-1} at 40 °C and ambient pressure. The open symbols refer to four independent experiments in solution of H_2O, whereas the filled squares refer to SP−PLP−NIR experiments on AMPS in solution of D_2O.

to laser pulsing at $t = 0$. Fitting of experimental monomer concentration vs time traces yields the kinetic parameters $k_p/\langle k_t \rangle$ and $\langle k_t \rangle c_R^0$. If either k_p or c_R^0 is known, individual $\langle k_t \rangle$ values may be calculated from $k_p/\langle k_t \rangle$ or $\langle k_t \rangle c_R^0$, respectively. Mostly, k_p is accessible from PLP−SEC experiments, for which reason the coupled parameter $\langle k_t \rangle / k_p$ is of particular interest.

The solid line in Figure 4 represents the fit of the measured AMPS conversion vs time data to eq 1. As can be seen from the plot of residuals in the lower part of Figure 4, a very satisfactory fit is obtained within the time interval up to 0.2 s, in which free-radical chain length increases up to about a few thousand monomer units. A single value of $\langle k_t \rangle$ thus affords a reasonable representation of the measured data. This observation should, however, not be taken as proof of ideal polymerization kinetics with $\langle k_t \rangle$ (and k_p) being independent of chain length. Explanations for the apparent chain-length independence of $\langle k_t \rangle$ are the following: (i) the chain-length dependence is rather weak and thus is difficult to detect within the limits of experimental accuracy; (ii) chain transfer to monomer is fast, which rapidly transforms the narrow chain-length distribution of radicals, which is characteristic of a perfect single laser pulse experiment, into a broad chain-length distribution that is adequately represented by a single average $\langle k_t \rangle$ value; (iii) frequent intramolecular hydrogen transfer, such as backbiting via a six-membered transition structure, takes place, which process would also result in a broad size distribution of radicals and in a single average $\langle k_t \rangle$ value being suitable for describing termination kinetics. The difficulties met in PLP−SEC investigations into k_p of AMPS indicate[16] that arguments (ii) and (iii) may indeed play a major role.

Satisfactory representations of measured SP−PLP−NIR traces by eq 1, similar to the one demonstrated in Figure 4, are obtained for the entire set of experiments carried out at other polymerization temperatures, other AMPS concentrations, and other degrees of monomer conversion and pH values. Thus, no reason is seen for using more refined kinetic models, e.g., expressions that include chain-length-dependent termination, to fit the SP−PLP−NIR traces. Equation 1 has been used for representing AMPS conversion vs time traces throughout this study.

The variation of $\langle k_t \rangle / k_p$ with the degree of monomer conversion, as obtained from a series of SP−PLP−NIR experiments at 40 °C with an initial AMPS concentration of 2.79 mol·L^{-1}, is depicted in Figure 5. The open symbols refer to experiments in H_2O, whereas the filled squares are data from SP−PLP−NIR experiments on AMPS dissolved in D_2O. The close agreement of $\langle k_t \rangle / k_p$ data obtained in solution of H_2O and of D_2O supports the expectation that this kind of solvent change does not affect polymerization rate coefficients. Up to 90% monomer conversion, $\langle k_t \rangle / k_p$ decreases only by about 0.2 logarithmic unit. A steeper decrease is seen above 90%, where a lowering of $\langle k_t \rangle / k_p$ by about 1 order of magnitude is found. The variation with monomer concentration of $\langle k_t \rangle / k_p$ for AMPS polymerization in aqueous phase is minor, if compared with methyl methacrylate bulk polymerization where $\langle k_t \rangle / k_p$ and $\langle k_t \rangle$ decrease by several orders of magnitude.[21] With dodecyl acrylate and dodecyl methacrylate bulk polymerizations, on the other hand, $\langle k_t \rangle$ stays constant within the entire conversion range studied so far, that is, up to about 80%. This type of behavior has been assigned to segmental diffusion control of termination kinetics.[3,22] Slight reductions in $\langle k_t \rangle$ toward higher degrees of monomer conversion occur in systems where k_t is controlled by reaction diffusion (RD),[23] e.g., in the bulk polymerizations of ethene and of butyl acrylate.[24] Under RD control, center-of-mass termination essentially occurs via monomer addition (propagation) steps in conjunction with reorientational motions of chain segments of the two macroradicals. The expression for a RD-controlled termination rate coefficient, $k_{t,RD}$, reads[24]

$$k_t = k_{t,RD} = C_{RD} k_p (1 - x) \tag{2}$$

in which x is monomer conversion and C_{RD} is the reaction diffusion constant which is obtained from an experimental $\langle k_t \rangle / k_p$ value measured under RD control of k_t at any precisely known monomer conversion x according to eq 3:

$$C_{RD} = \frac{k_{t,RD}}{k_p (1 - x)} \tag{3}$$

Analysis of the conversion dependence of $\langle k_t \rangle / k_p$ (Figure 5) according to eq 2, under the assumption that C_{RD} and k_p are independent of monomer conversion, tells that the decrease of $\log(\langle k_t \rangle / k_p)$ up to 90% monomer conversion is too small to be assigned to RD control. Equation 2 predicts a lowering by 1 order of magnitude ($\Delta \log(\langle k_t \rangle / k_p) = -1$) between 0 and 90% monomer conversion. On the other hand, the significantly larger decrease in experimental $\langle k_t \rangle / k_p$ data above 90% conversion is not in conflict with assuming RD control of k_t, as eq 2 is associated with a lowering in $\langle k_t \rangle / k_p$ by another order of magnitude between 90 and 99% monomer conversion.

a. Temperature Dependence of $\langle k_t \rangle / k_p$. SP−PLP−NIR experiments with an initial AMPS concentration of 2.79 mol·L^{-1} have also been carried out at 10 and 25 °C. The resulting $\langle k_t \rangle / k_p$ values are presented in Figure 6, which also contains the data points measured in H_2O solution at 40 °C (see Figure 5). The data for 25 and 40 °C sit on top of each other and are in close agreement with the values for 10 °C. Because of the enhanced scatter of the 10 °C data, but also because of the narrow experimental temperature range, it cannot be decided whether $\langle k_t \rangle / k_p$ is independent of temperature, which has been identified as a signature of termination under RD control in ethene and butyl acrylate polymerization.[25]

b. Influence of pH on $\langle k_t \rangle / k_p$. In contrast to the weak acids acrylic acid and methacrylic acid, the strong sulfonic acid AMPS is completely deprotonated in aqueous solution at its natural pH. Neutralization does not increase the degree of ionization. Thus pH variation is not expected to result in similarly large effects on rate coefficients, as have been observed for acrylic acid[13] and methacrylic acid[16] homopolymerizations. The pH of an aqueous 2.79 mol·L^{-1} AMPS solution is below 0, and pH 7

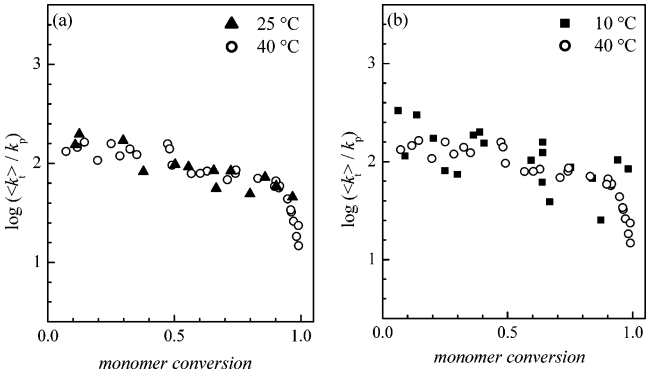

Figure 6. Dependence on monomer conversion of $\langle k_t \rangle / k_p$ for aqueous 2-acrylamido-2-methylpropanesulfonic acid polymerizations at initial monomer concentration of 2.79 mol·L^{-1}: (a) experimental data for 25 and 40 °C; (b) experimental data for 10 and 40 °C.

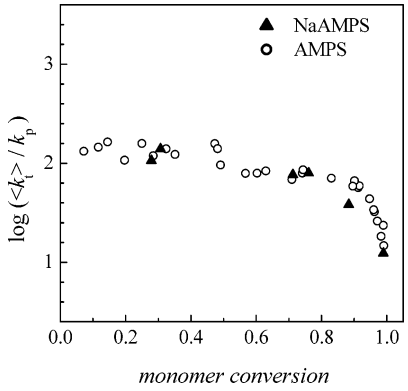

Figure 7. Dependence on monomer conversion of $\langle k_t \rangle / k_p$ for homopolymerizations in aqueous 2.79 mol·L^{-1} solutions of 2-acrylamido-2-methylpropanesulfonic acid (AMPS) and sodium salt of AMPS (NaAMPS) at 40 °C.

is found for the aqueous solution of the sodium salt of AMPS (NaAMPS). Moreover, as also poly(AMPS) is a strong polyelectrolyte,[26] the charges of all three relevant species of AMPS polymerization—monomer, macroradical, and polymer—are not effectively screened by counterions up to very high salt concentrations.

Figure 7 shows $\langle k_t \rangle / k_p$ data for NaAMPS and for AMPS polymerizations, both at 2.79 mol·L^{-1} and 40 °C. As with AMPS, the aqueous solution polymerization of NaAMPS may be run in homogeneous liquid phase up to almost complete monomer conversion. Within experimental accuracy the $\langle k_t \rangle / k_p$ values for NaAMPS and for AMPS at the same monomer conversion are identical, which is most likely due to the fact that the same monomer and radical species occur in both systems. This agreement of kinetic data for acid and salt forms seems to indicate the strong polyelectrolyte character of poly(AMPS) since no screening effect of sodium counterions at the relatively high concentration of 2.79 mol·L^{-1} is present.

c. Influence of Monomer Concentration on $\langle k_t \rangle / k_p$. Using D_2O instead of H_2O as the solvent allows for SP−PLP−NIR experiments at lower AMPS concentrations. Shown in Figure 8 are $\langle k_t \rangle / k_p$ data measured during an AMPS polymerization at 40 °C and 1.04 mol·L^{-1} initial monomer concentration. The data taken on the 2.79 mol·L^{-1} aqueous AMPS solution are presented for comparison. Throughout the experimental monomer conversion range up to 90%, $\langle k_t \rangle / k_p$ for 1.04 mol·L^{-1} is above the values measured on the 2.79 mol·L^{-1} solution for identical monomer conversion, by a factor $F = 6.5$ at 30% monomer conversion, $F = 5.1$ at 70% conversion, and $F = 4.5$ at 90% monomer conversion. The solid line through the data

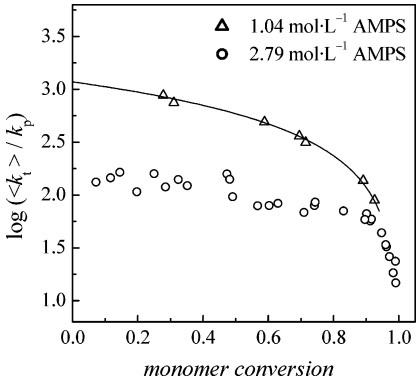

Figure 8. Dependence on monomer conversion of $\langle k_t \rangle / k_p$ for 2-acrylamido-2-methylpropanesulfonic acid (AMPS) polymerizations at 40 °C and two initial AMPS concentrations: 2.79 mol·L^{-1} (dissolved in H_2O) and 1.04 mol·L^{-1} (dissolved in D_2O). The photoinitiator concentration was $c_{Darocur} = 5 \times 10^{-3}$ mol·L^{-1}. The line represents a fit of the data at lower AMPS content (1.04 mol·L^{-1}) to eq 2.

points for $\langle k_t \rangle / k_p$ at 1.04 mol·L^{-1} illustrates the fit to eq 2, which provides a remarkably good representation of $\langle k_t \rangle / k_p$ over the extended experimental monomer conversion range from 27 to 92%. Thus termination rate control by reaction diffusion may be operative at this lower AMPS content. The associated C_{RD} value is slightly above 1000, as may be read from the intersection point of the fitted line with the ordinate in Figure 8 (see eq 3 for $x = 0$). C_{RD} values of this size have been found for RD-controlled termination in acrylate homopolymerization at ambient pressure.[25] Despite this agreement, the $\langle k_t \rangle / k_p$ data for an AMPS content of 1.04 mol·L^{-1} provide no proof for termination by RD. The data in Figure 8, however, demonstrate that RD according to eq 2, with a single RD constant C_{RD}, is not capable of adequately representing termination at both AMPS contents, 1.04 and 2.79 mol·L^{-1}. This is seen by inspection of the effect of changing AMPS content and AMPS conversion on $\langle k_t \rangle / k_p$. At low initial AMPS concentration a steady decrease of $\langle k_t \rangle / k_p$ with conversion is seen, which is consistent with termination being determined by RD: due to the lowering of AMPS concentration with conversion, the propagation rate is lowered, which affects termination via RD. On the other hand, increasing the AMPS concentration, by choosing the initial AMPS content to be 2.79 mol·L^{-1}, also reduces $\langle k_t \rangle / k_p$ and does so to a significant extent, which is not what one expects in case of RD control. In addition, up to a monomer conversion of 90%, only a minor decrease of $\langle k_t \rangle / k_p$ with conversion occurs at 2.79 mol·L^{-1}. These findings suggest that k_t is not controlled by RD at this higher initial AMPS concentration.

In situations where RD control does not apply, the correlation of $\langle k_t \rangle$ and k_p, via eq 2, is lost and both rate parameters need to be treated as independent quantities. Under such conditions particular interest focuses on the individual rate coefficients $\langle k_t \rangle$ and k_p. Application of PLP−SEC conditions similar to those used in our previous work on ionized acrylic acid[13] did not result in structured molecular weight distributions suitable for k_p evaluation, although temperatures, monomer concentrations, and photoinitiator concentrations were varied over a wide range and different photoinitiators were used. As for PLP−SEC experiments of acrylic acid or acrylate monomers, these problems may be due to the occurrence of chain-transfer events.[37] In addition, the EPR spectroscopic method for k_p determination[17] is not easily applicable in aqueous phase. Therefore, chemically initiated polymerizations of AMPS in aqueous solution have been carried out to provide access to individual $\langle k_t \rangle$ and k_p values.

Chemically Initiated AMPS Polymerization. Using SP−PLP−NIR in conjunction with chemically initiated polymerization for deducing $\langle k_t \rangle$ and k_p from the coupled parameters $\langle k_t \rangle / k_p$ and $\langle k_t \rangle / k_p^2$ runs into problems when the average size and size distribution of radicals are significantly different within the two types of experiments.[17,27] This effect may at least partly contribute to the wide scatter in tabulated k_p and $\langle k_t \rangle$ data reported for one and the same monomer under ostensibly the same polymerization conditions.[28] A detailed discussion of this topic is beyond the scope of this paper, and the reader is referred to the literature.[17,27−31] In AMPS polymerizations, differences in size and size distribution of radicals may not pose severe problems. This is indicated by the rather satisfactory representation of the SP−PLP−NIR trace in Figure 4 by eq 1, which uses just one termination rate coefficient to fit conversion vs time traces referring to a wide range of chain lengths. An advantage of using SP−PLP−NIR in conjunction with chemical initiation, rather than with PLP−SEC, relates to the fact that both experiments may be carried out over an extended monomer conversion range. PLP−SEC only delivers k_p for low degrees of monomer conversion. This value is used for kinetic analysis over the entire conversion range for which information from SP−PLP−NIR is available.

Chemically initiated polymerizations were carried out at 40 °C and ambient pressure on aqueous solutions at initial AMPS concentrations of 1.04 and 2.79 mol·L^{-1}. The concentration of the initiator $Na_2S_2O_8$ was chosen to be 0.02 mol·L^{-1}. Monomer conversion, c_M, as a function of polymerization time was monitored via in-line FT-NIR spectroscopy. The resulting $c_M(t)$ data were analyzed according to eq 4:

$$r_p = -\frac{dc_M}{dt} = c_M k_p \left(\frac{f k_d c_I}{\langle k_t \rangle} \right)^{0.5} \tag{4}$$

with the initiator decomposition rate coefficient k_d, the initiator concentration c_I, and the initiator efficiency f, which latter quantity characterizes the fraction of the radicals from initiator decomposition that adds to a monomer molecule and thus starts macromolecular growth. Inspection of eq 4 tells that deducing $\langle k_t \rangle^{0.5}/k_p$ (or $\langle k_t \rangle / k_p^2$) from chemically induced polymerization experiments requires f and k_d or the product fk_d to be known. For experiments that have been carried out over a range of monomer conversions, it further needs to be known whether and to what extent f varies with monomer conversion. Within the present study it is assumed that f is independent of monomer conversion, at least within the intermediate monomer concentration range from 25 to 70%. This assumption is supported by studies into the conversion dependence of the efficiency that yield almost constant f up to at least 80% conversion in bulk homopolymerizations of styrene and methyl methacrylate.[32,33]

For deducing $\langle k_t \rangle^{0.5}/k_p$ from the chemically initiated AMPS polymerizations, the f and k_d values reported for $Na_2S_2O_8$-induced heterogeneous polymerization of styrene and methyl methacrylate were adopted:[34,35] $f = 1$ and $k_d = 2.3 \times 10^{-7}$ s^{-1}. These values refer to neutral conditions, whereas the AMPS polymerizations reported here were carried out at pH <0. The results for $\langle k_t \rangle / k_p^2$ are plotted vs monomer conversion in Figure 9. Data at lower conversion have not been included in Figure 9, as traces of impurities may affect polymerization kinetics in the early reaction period. The variation of $\langle k_t \rangle / k_p^2$ with monomer conversion is relatively weak.

A particularly remarkable observation from Figure 9 is that $\langle k_t \rangle / k_p^2$ is more or less identical for the two AMPS concentrations, whereas $\langle k_t \rangle / k_p$ significantly differs for these two concentrations, as can be seen from Figure 8. $\langle k_t \rangle / k_p$ was higher at lower AMPS concentration by a factor F, which slightly decreased toward higher monomer conversion, e.g., from $F = 6.5$ at 30% conversion to $F = 4.5$ at 90% conversion (see above). For a given degree of monomer conversion the observations from Figures 8 and 9 may be expressed by

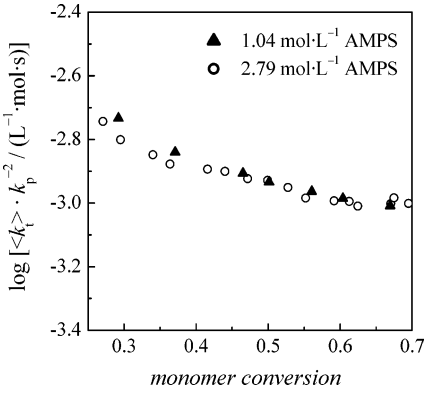

Figure 9. Dependence on conversion of $\langle k_t \rangle / k_p^2$ for chemically initiated polymerizations of 2-acrylamido-2-methylpropanesulfonic acid (AMPS) dissolved in water at two AMPS contents: 2.79 mol·L^{-1} (circles) and 1.04 mol·L^{-1} (triangles). The polymerizations were carried out at 40 °C, ambient pressure, and initiator concentrations of 0.02 mol·L^{-1}.

$$\frac{\langle k_{t,1} \rangle}{k_{p,1}^2} = \frac{\langle k_{t,2} \rangle}{k_{p,2}^2} \tag{5}$$

and

$$\frac{\langle k_{t,1} \rangle}{k_{p,1}} = F \frac{\langle k_{t,2} \rangle}{k_{p,2}} \tag{6}$$

where the subscripts "1" and "2" refer to AMPS concentrations of 1.04 mol·L^{-1} and 2.79 mol·L^{-1}, respectively. Combining eqs 5 and 6 yields

$$k_{p,1} = F k_{p,2} \tag{7}$$

and

$$\langle k_{t,1} \rangle = F^2 \langle k_{t,2} \rangle \tag{8}$$

With F being well above unity, eqs 7 and 8 indicate that for the specific situation of aqueous-phase AMPS polymerization, upon increasing monomer concentration, k_p drops by a factor of F and k_t by a factor of F^2. This observation may be understood as resulting from reaction diffusion control of k_t (see eq 2; $k_t = k_{t,RD} = C_{RD} k_p (1 - x)$). k_t scales with both k_p and with the reaction diffusion constant C_{RD}, which both appear to be lowered as a consequence of restricted chain mobility toward increasing AMPS concentration (and thus decreasing water content), as will be discussed in more detail below.

Combining $\langle k_t \rangle / k_p^2$ and $\langle k_t \rangle / k_p$ values measured for identical AMPS content, AMPS conversion, temperature, and pH yields the individual k_p and $\langle k_t \rangle$ values for 40 °C plotted in Figure 10. The data are presented as a function of monomer conversion for the two AMPS contents of 1.04 and 2.79 mol·L^{-1}. Within the 25−70% monomer conversion region, k_p turns out to be independent of conversion. On the other hand, k_p is clearly different, by about a factor of 4, at the two AMPS contents.

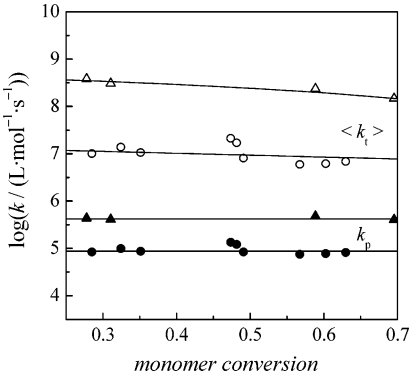

Figure 10. Dependence on monomer conversion of k_p (filled symbols) and $\langle k_t \rangle$ (open symbols) for 2-acrylamido-2-methylpropanesulfonic acid (AMPS) polymerization at 40 °C, ambient pressure, and two initial AMPS concentrations: 1.04 mol·L^{-1} (triangles) and 2.79 mol·L^{-1} (circles).

The propagation rate coefficients obtained as arithmetic means of log k_p are

$$\log(k_p/\text{L·mol}^{-1}\text{·s}^{-1}) = 5.6 \pm 0.2$$

for 1.04 mol L^{-1} AMPS solution

and

$$\log(k_p/\text{L·mol}^{-1}\text{·s}^{-1}) = 4.9 \pm 0.2$$

for 2.79 mol L^{-1} AMPS solution

The $\langle k_t \rangle$ values for the lower AMPS content are significantly, by more than 1 order of magnitude, above the ones at the higher AMPS content. Moreover, $\langle k_t \rangle$ decreases toward higher monomer conversion, with this effect being larger for the 1.04 mol·L^{-1} aqueous AMPS solution.

If the actual efficiency (or the product fk_d) differed from the adopted value by a factor of 2, this would not result in major changes of the log k_p and log $\langle k_t \rangle$ plots in Figure 10. Thus, if the efficiency were 0.5 instead of 1.0, the resulting change would be an increase in log k_p by 0.3 logarithmic unit. If the actual f and/or fk_d values differed from the adopted ones by as much as a factor of 10, the resulting change of k_p and k_t would be by 1 logarithmic unit, with these changes occurring to higher rate values in the case that f and/or fk_d drops. It should further be noted that the uncertainty in fk_d does not affect the relative size of k_p to k_t for a given AMPS content, nor the relative size of k_p and of k_t values referring to the two AMPS concentrations (in the case that fk_d is not dependent on AMPS content).

The AMPS k_p values (Figure 10) are of the same order of magnitude as the recently reported k_p values for acrylic acid[12,14] and acrylamide[10] in aqueous solution. For example, for acrylic acid polymerizations at 25 °C and a monomer concentration of 0.4 mol·L^{-1}, k_p values up to 180 000 L·mol^{-1}·s^{-1} were reported.[12,14] With an activation energy of 12 kJ·mol^{-1}, a k_p value of 227 000 L·mol^{-1}·s^{-1} is estimated for 40 °C, which is not too far from the k_p values determined for AMPS in this work. Rather high k_p values were also reported by the group of Gilbert for aqueous-phase polymerizations of acrylamide: e.g., k_p = 104 000 L·mol^{-1}·s^{-1} at 40 °C for a monomer concentration of 0.32 mol·L^{-1}.[10]

Also in agreement with results from studies into aqueous-phase polymerizations of other water-soluble monomers is the significant lowering of k_p toward increasing monomer concentration. Effects on k_p may be due to the "local" monomer concentration at the free-radical site being dissimilar to the known overall monomer concentration.[14] Such arguments were very helpful in interpreting the variation of k_p with monomer concentration in (meth)acrylate−CO_2 mixtures.[36] The variation of AMPS k_p with monomer concentration depicted in Figure 10, however, appears to be too large for being essentially assigned to such a "local" monomer concentration effect. Another explanation assumes that, toward higher monomer conversion, intermolecular chain-transfer processes produce significant fractions of midchain radicals with the associated propagation reaction from the midchain position being significantly below the k_p of radicals with the functionality at the chain-end position.[37] If this effect were the dominant one, a strong dependence of k_p on monomer conversion would be expected, as intermolecular chain transfer is enhanced toward higher polymer content. No such dependence, however, can be detected for the k_p data in Figure 10. A third explanation is related to the finding from a recent study by our group that revealed a 10-fold decrease in k_p for nonionized methacrylic acid (MAA) in going from very dilute solution to the bulk system.[38] The decrease in k_p was assigned to a decrease in the preexponential factor, A, of k_p. The lowering of $A(k_p)$ is due to intermolecular interactions between the transition state (TS) structure for MAA propagation and an MAA environment being significantly stronger than the ones between the TS structure and an H_2O environment. In an MAA-rich environment the barrier to rotational motion of the relevant degrees of motions of the TS thus experiences enhanced friction, which is associated with a lowering of the preexponential factor and thus of k_p. Such a reduction of chain mobility toward higher monomer content also seems to be the most likely explanation for the AMPS system. In addition to a restriction of chain mobility by intermolecular interactions, in the case of AMPS also intramolecular interactions due to repulsion between the anionic moieties on the polymer chain may play a role. AMPS polymerized up to high conversions at the initial AMPS concentrations used in this work leads to the formation of polyelectrolyte chains in concentrated or even swollen solution regimes[39] from the very beginning of the polymerization. The experimental and theoretical work on polyelectrolytes in solution has been mainly devoted to dilute and semidilute regimes, which, depending on the molecular weight, type of polymer, and ionic strength, range at most up to a few weight percent of polyelectrolyte in solution.[40,41] In addition, these studies refer to binary systems of polymer and water without monomer being present as cosolvent. An adequate description of polyelectrolyte behavior in the higher concentration regimes and in the presence of salt, i.e., under realistic polymerization conditions for the conversion ranges shown in Figures 9 and 10 at both AMPS concentrations, is missing so far. Thus, results from these studies cannot directly be transferred to our polymerization system.

The assumption of reduced mobility of polyelectrolyte chains formed at the higher monomer concentration (2.79 mol·L^{-1}), associated with a 2.7-fold higher polymer content than is present at the same conversion in the polymerization at the lower monomer content (1.04 mol·L^{-1}), also helps in qualitatively understanding the k_t behavior of AMPS. At the lower monomer content k_p is remarkably large, around 4×10^5 L·mol^{-1}·s^{-1}, which favors termination by reaction diffusion (eq 2). Higher chain mobility is also associated with a larger reaction diffusion constant, C_{RD}, which additionally favors RD. The value of $C_{RD}^0 = C_{RD}/c_{AMPS}^0$ = 1130 L·mol^{-1} (where c_{AMPS}^0 is the initial monomer concentration) that is obtained from fitting the $\langle k_t \rangle/k_p$ or $\langle k_t \rangle$ data for 1.04 mol·L^{-1} to eq 2, is in close agreement with numbers obtained for acrylate termination under RD control.[25]

Thus, it is not unexpected that the RD mechanism provides an adequate representation of the $\langle k_t \rangle / k_p$ data (Figure 8) and of the $\langle k_t \rangle$ data (Figure 10) for the lower AMPS content of 1.04 mol·L^{-1}. The lines through the $\langle k_t \rangle / k_p$ and $\langle k_t \rangle$ data points for 1.04 mol·L^{-1} are fits according to the RD expression in eq 2.

At the higher AMPS content of 2.79 mol·L^{-1}, k_p is distinctly lower (see Figure 10). If reduced chain mobility is the correct explanation for this decrease, also C_{RD} should be significantly lower (see Figure 8), as the free radicals are less capable of rearrangement and of exploring their molecular environment, and thus of approaching other free-radical functionalities. Whether termination at the AMPS content of 2.79 mol·L^{-1} should be assigned to a less efficient reaction diffusion, e.g., with C_{RD} being dependent on monomer conversion, or to a different mechanism cannot be decided on the basis of the presently available experimental material. Further experiments need to be carried out in a wider range of AMPS contents and upon significant variation of ionic strength.

Conclusions

Within the present investigation termination and propagation rate coefficients for aqueous AMPS polymerizations were determined. For the first time, the SP−PLP−NIR technique has been used in conjunction with chemically initiated polymerization to deduce rate coefficients of propagation and termination. The experiments were carried out at 40 °C and monomer contents of 20 and 50 wt % with the polymerizations being followed up to almost complete monomer conversion. High signal-to-noise quality of the SP−PLP−NIR experiment at low monomer contents could be achieved by AMPS polymerization in solution of D_2O.

k_p is significantly higher at the lower AMPS content, but no variation with monomer conversion can be detected, at least not up to conversions of 70%. k_t is also significantly higher at lower AMPS content, but shows a slight decrease with monomer conversion. The k_t behavior at the lower AMPS content may be understood in terms of reaction diffusion control. The rate coefficients measured during polymerization of the 50 wt % aqueous AMPS solution are indicative of a polyelectrolyte effect that reduces chain mobility.

Acknowledgment. P.H. acknowledges a fellowship by the Fonds der Chemischen Industrie. Financial support by the Deutsche Forschungsgemeinschaft within the framework of the European Graduate School "Microstructural Control in Free Radical Polymerization" and by BASF AG is gratefully appreciated. We are grateful to the reviewer who suggested the introduction of the arguments contained in eqs 5−8.

References and Notes

(1) Beuermann, S.; Buback, M. *Prog. Polym. Sci.* **2002**, *27*, 191−254.
(2) Buback, M.; Hippler, H.; Schweer, J.; Vögele, H.-P. *Makromol. Chem., Rapid Commun.* **1986**, *7*, 261−265.
(3) Buback, M.; Kowollik, C. *Macromolecules* **1999**, *32*, 1445−1452.
(4) Buback, M.; Feldermann, A. *Aust. J. Chem.* **2002**, *55*, 475−481.
(5) Buback, M.; Egorov, M.; Feldermann, A. *Macromolecules* **2004**, *37*, 1768−1776.
(6) Beuermann, S.; Buback, M.; Schmaltz, C. *Ind. Eng. Chem. Res.* **1999**, *38*, 3338−3344.
(7) Smith, G. B.; Russell, G. T.; Yin, M.; Heuts, J. P. A. *Eur. Polym. J.* **2005**, *41*, 225−230.
(8) Olaj, O. F.; Bitai, I.; Hinkelmann, F. *Makromol. Chem.* **1987**, *188*, 1689−1702.
(9) Ganachaud, F.; Balic, R.; Monteiro, M. J.; Gilbert, R. G. *Macromolecules* **2000**, *33*, 8589−8596.
(10) Seabrook, S. A.; Tonge, M. P.; Gilbert, R. G. *J. Polym. Sci., Polym. Chem. Ed.* **2005**, *43*, 1357−1368.
(11) Kuchta, F.-D.; van Herk, A. M.; German, A. L. *Macromolecules* **2000**, *33*, 3641−3649.
(12) Lacík, I.; Beuermann, S.; Buback, M. *Macromolecules* **2001**, *34*, 6224−6228.
(13) Lacík, I.; Beuermann, S.; Buback, M. *Macromol. Chem. Phys.* **2004**, *205*, 1080−1087.
(14) Lacík, I.; Beuermann, S.; Buback, M. *Macromolecules* **2003**, *36*, 9355−9363.
(15) Gong, J. P.; Kurokawa, T.; Narita, T.; Kagata, G.; Osada, Y.; Nishimura, G.; Kinjo, M. *J. Am. Chem. Soc.* **2001**, *123*, 5582−5583.
(16) Hesse, P. Diploma Thesis, Göttingen, 2004.
(17) Buback, M.; Gilbert, R. G.; Russell, G. T.; Hill, D. J.; O'Driscoll, K. F.; Shen, J.; Winnik, M. A. *J. Polym. Sci., Polym. Chem. Ed.* **1992**, *30*, 851−863.
(18) Buback, M.; Hinton, C. In *High-Pressure Techniques in Chemistry and Physics*; Holzapfel, W. B., Isaacs, N. S., Eds.; Oxford University Press: Oxford, UK, 1997; p 151.
(19) Buback, M. *Angew. Chem., Int. Ed. Engl.* **1991**, *30*, 641−653.
(20) Buback, M.; Huckestein, B.; Kuchta, F.-D.; Russell, G. T.; Schmid, E. *Macromol. Chem. Phys.* **1994**, *195*, 2117−2140.
(21) Sack-Kouloumbris, R.; Meyerhoff, G. *Makromol. Chem.* **1989**, *190*, 1133−1152.
(22) Benson, S. W.; North, A. M. *J. Am. Chem. Soc.* **1962**, *84*, 935−940.
(23) Schulz, G. V. *Z. Phys. Chem. (Munich)* **1956**, *8*, 290−317.
(24) Buback, M. *Makromol. Chem.* **1990**, *191*, 1575−1587.
(25) Buback, M.; Huckestein, B.; Russell, G. T. *Macromol. Chem. Phys.* **1994**, *195*, 539−554.
(26) Gooda, S. R.; Huglin, M. B. *J. Polym. Sci., Part A* **1992**, *30*, 1549−1557.
(27) Olaj, O. F.; Kornherr, A.; Zifferer, G. *Macromol. Theory Simul.* **2000**, *9*, 131−140.
(28) *Polymer Handbook*, 4th ed.; Brandrup, J., Immergut, E. H., Grulke, E. A., Eds.; Wiley: New York, 1999; pp II/77−II/95.
(29) Buback, M.; Egorov, M.; Gilbert, R. G.; Kaminsky, V.; Olaj, O. F.; Russell, G. T.; Vana, P.; Zifferer, G. *Macromol. Chem. Phys.* **2002**, *203*, 2570−2582.
(30) Barner-Kowollik, C.; Buback, M.; Egorov, M.; Fukuda, T.; Goto, A.; Olaj, O. F.; Russell, G. T.; Vana, P.; Yamada, B.; Zetterlund P. *Prog. Polym. Sci.* **2005**, *30*, 605−643.
(31) Russell, G. T. *Aust. J. Chem.* **2002**, *55*, 399−414.
(32) Carswell, T. G.; Hill, D. J. T.; Londero, D. I.; O'Donnell, J. H.; Pomery, P. J.; Winzor, C. L. *Polymer* **1992**, *33*, 137−140.
(33) Zetterlund, P. B.; Yamazoe, H.; Yamada, B.; Hill, D. J. T.; Pomery, P. J. *Macromolecules* **2001**, *34*, 7686−7691.
(34) Russell, G. T. Private communication, 2004.
(35) Behrmann, E. J.; Edwards, J. O. *Rev. Inorg. Chem.* **1980**, *3*, 179−206.
(36) Beuermann, S.; Buback, M.; El Rezzi, V.; Jürgens, M.; Nelke, D. *Macromol. Chem. Phys.* **2004**, *205*, 876−883.
(37) Asua, J. M.; Beuermann, S.; Buback, M.; Castignolles, P.; Charleux, B.; Gilbert, R. G.; Hutchinson, R. A.; Leiza, J. R.; Nikitin, A. N.; Vairon, J.-P.; van Herk, A. M. *Macromol. Chem. Phys.* **2004**, *205*, 2151−2160.
(38) Beuermann, S.; Buback, M.; Hesse, P.; Lacík, I. *Macromolecules*, **2006**, *39*, 184−193.
(39) Nishida, K.; Kaji, K.; Kanaya, T. *J. Chem. Phys.* **2001**, *115*, 8217−8220.
(40) Dautzenberg, H.; Jaeger, W.; Kötz, J.; Philipp, B.; Seidel, C.; Stscherbina, D. Characterization of macromolecular parameters in polyelectrolyte solutions. In *Polyelectrolytes: Formation, Characterization and Application*; Hauser Publishers: Munich, Vienna, New York, 1994; Chapter 5, p 166.
(41) Sedlák, M. *Langmuir* **1999**, *15*, 4045−4051.

MA051187N